Heliyon 10 (2024) e36061

Contents lists available at ScienceDirect

Heliyon

journal homepage: www.cell.com/heliyon

Research article

Non-invasive TMS attenuates neuropathic pain after spinal cord injury associated with enhancing brain functional connectivity and HPA axis activity

Qing Zhao [a,b,c,1], Lijuan Zhao [a,b,1], Pianpian Fan [d,1], Yanjing Zhu [b], Rongrong Zhu [b,**], Liming Cheng [a,b,e,***], Ning Xie [a,b,2,*]

[a] Division of Spine, Department of Orthopedics, Tongji Hospital, Tongji University School of Medicine, Tongji University, Shanghai, 200065, China
[b] Key Laboratory of Spine and Spinal Cord Injury Repair and Regeneration of Ministry of Education, Orthopaedic Department of Tongji Hospital, School of Medicine, School of Life Sciences and Technology, Tongji University, Shanghai, 200065, China
[c] Department of Spine Surgery, Center for Orthopaedic Surgery, Academy of Orthopedics, Orthopaedic Hospital of Guangdong Province, The Third Affiliated Hospital of Southern Medical University, Guangzhou, 510665, China
[d] Department of Pediatrics, West China Second Hospital, Sichuan University, Chengdu, 610044, China
[e] Clinical Center for Brain and Spinal Cord Research, Tongji University, Shanghai, 200065, China

ARTICLE INFO

Keywords:
Spinal cord injury
Neuropathic pain
Transcranial magnetic stimulation (TMS)
Brain functional connectivity
Hypothalamic pituitary adrenal (HPA) axis
Early intervention

ABSTRACT

Patients with spinal cord injury (SCI) often suffer from varying degrees of neuropathic pain.

Non-invasive repetitive transcranial magnetic stimulation (TMS) has been shown to improve neuropathic pain, while the appropriate intervention strategies of TMS treatment and how TMS affects brain function after SCI were not entirely clear. To investigate the effects and mechanisms of TMS on neuropathic pain after SCI, high-frequency TMS on primary motor cortex (M1) of mice was performed after SCI and pain response was evaluated through an electronic Von-Frey device and cold/hot plates. Functional magnetic resonance imaging (fMRI), bulk RNA sequencing, immunofluorescence and molecular experiments were used to evaluate brain and spinal cord function changes and mechanisms. TMS significantly improved SCI induced mechanical allodynia, cold and thermal hyperalgesia with a durative effect, and TMS intervention at 1 week after SCI had pain relief advantages than at 2 weeks. TMS intervention not only affected the functional connections between the primary motor cortex and the thalamus, but also increased the close connection of multiple brain regions. Importantly, TMS treatment activated the hypothalamic pituitary adrenal (HPA) axis and increased the transcript levels of genes encode hormone proteins, accompanied with the attenuation of inflammatory microenvironment in spinal cord associated with pain relief. Totally, these results elucidate that early intervention with TMS could

* Corresponding author. Key Laboratory of Spine and Spinal Cord Injury Repair and Regeneration of Ministry of Education, Division of Spine, Orthopaedic Department of Tongji Hospital, School of Medicine, Tongji University, 389 Xincun Rd, Shanghai, 200065, China.
** Corresponding author. Key Laboratory of Spine and Spinal Cord Injury Repair and Regeneration of Ministry of Education, Division of Spine, Orthopaedic Department of Tongji Hospital, School of Life Sciences and Technology, Tongji University, 389 Xincun Rd, Shanghai, 200065, China.
*** Corresponding author. Key Laboratory of Spine and Spinal Cord Injury Repair and Regeneration of Ministry of Education, Division of Spine, Orthopaedic Department of Tongji Hospital, School of Medicine, Tongji University, 389 Xincun Rd, Shanghai, 200065, China.
E-mail addresses: rrzhu@tongji.edu.cn (R. Zhu), limingcheng@tongji.edu.cn (L. Cheng), nxieprof18@tongji.edu.cn (N. Xie).
[1] Equal first author.
[2] Lead Contact.

https://doi.org/10.1016/j.heliyon.2024.e36061
Received 7 May 2024; Received in revised form 23 July 2024; Accepted 8 August 2024
Available online 10 August 2024

improve neuropathic pain after SCI associated with enhancing brain functional connectivity and HPA axis activity which should be harnessed to modulate neuropathic pain after SCI.

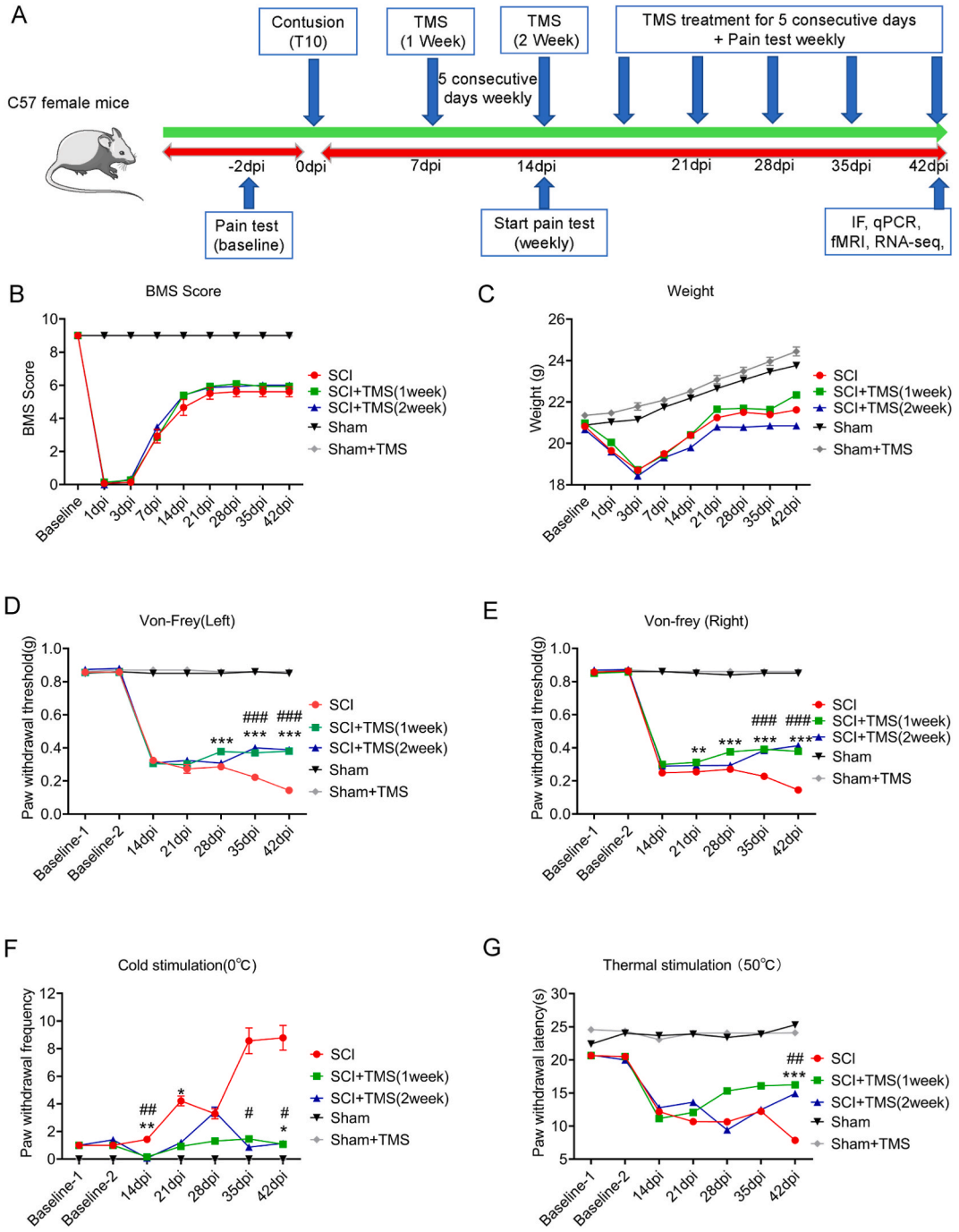

Fig. 1. TMS attenuated SCI induced neuropathic pain.
(**A**), the experimental flow chart. Change of BMS scores (**B**), weight (**C**), mechanical allodynia (**D-E**), cold hyperalgesia (**F**) and thermal hyperalgesia (**G**) in mice after TMS treatment at different time. Sham group, n = 10; Sham + TMS group, n = 5; SCI group, n = 15; SCI + TMS (1week) group, n = 15; SCI + TMS (2week) group, n = 15. Left, left hindlimbs; right, right hindlimbs. Values are the mean ± SEM. Statistical significance was determined by one-way ANOVA followed by Student Newman–Keuls post hoc test. *P < 0.05, **P < 0.01, ***P < 0.001, SCI + TMS (1 week) group VS. SCI group. $^{\#}$P < 0.05, $^{\#\#}$P < 0.01, $^{\#\#\#}$P < 0.001, SCI + TMS (2 week) group VS. SCI group.

1. Introduction

In the clinic, approximately 65 % of patients with spinal cord injury (SCI) suffer from chronic, severe, and persistent neuropathic pain [1]. Unfortunately, the treatment effects for neuropathic pain are still limited [2]. Non-invasive brain stimulation methods, such as repetitive transcranial magnetic stimulation (TMS), have been used to treat neuropathic pain [3]. TMS is approved by the Food and Drug Administration (FDA) to treat a variety of central nervous system (CNS) related diseases, including chronic pain [4]. TMS relies on electromagnetic coils to generate a powerful magnetic field to modulate neuronal excitability [4] and relieve pain by modulating

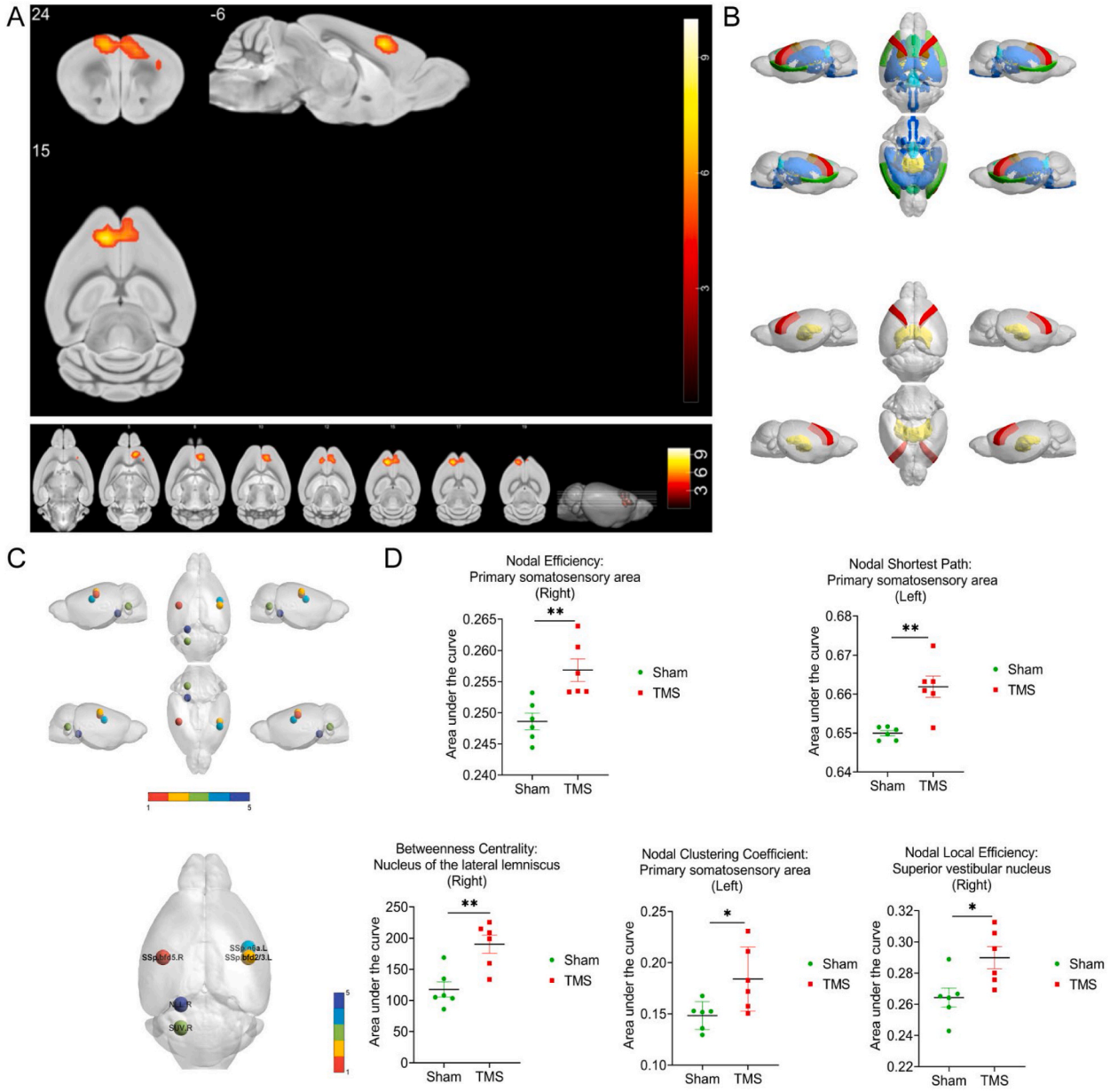

Fig. 2. Functional MRI revealed that TMS established a direct connection between the cortex and thalamus.
(**A**), TMS-related changes in regional homogeneity (ReHo) shown as a comparison between mice from TMS (SCI with TMS treatment, n = 3) and control groups (SCI without TMS treatment, n = 3) during the resting state. T score bars are shown. Warm colors indicate ReHo decreases in TMS group. (Chunk information: Secondary motor area, layer 4/5 Right; Number of voxels: 93; Peak MNI coordinate: −6, 21, 15; Peak intensity: −8.4926). (**B**), Schematic diagram of 7 ROIs. The primary motor cortex (MOp) - thalamus connectivity was significantly increased in mice of TMS group. (**C-D**), the color of nodes represents corresponding networks, including nodal efficiency, nodal local efficiency, betweenness centrality, nodal shortest path, local clustering coefficient. L, left; R, right. ROI, region of interest. Descriptive statistics are indicated as mean ± SD in all plots with a statistical significance level of $P < 0.05$. *P < 0.05, **P < 0.01, TMS group VS. control group.

various brain regions [3]. For chronic pain treatment, the primary target of TMS is the primary motor cortex (M1), and the best efficacy is achieved with lateral stimulation at high frequencies (5–20 Hz, 80 % of motor threshold) [3,5]. TMS treatment of peripheral neuropathic pain of the M1 area could attenuate pain sensory dimensions and self-reported pain intensity for over 25 weeks [3]. And daily high-frequency M1 TMS was found to be tolerable and provided temporary pain relief in patients with neuropathic pain [6]. However, the appropriate intervention strategies of TMS treatment and how TMS affects brain function and neuropathic pain after SCI were not entirely clear, which hinder the further clinical application of TMS in patients with SCI induced neuropathic pain.

Researchers have reported that TMS-induced analgesia is based on the remodeling of the endogenous opioid system and the restoration of normal cortical excitability, along with the inhibition of the transmission of nociceptive signals [5,7,8]. TMS-mediated analgesia maybe also through regulating the expression of inflammatory factors [5]. A previous study explored that active excitatory M1 TMS promoted pain recovery during the transition from acute to persistent pain [9]. Others demonstrated that M1 high-frequency TMS administered at 3-week intervals produced sustained analgesia, thus supporting the clinical interest in this stimulation paradigm in the treatment of refractory chronic pain [10]. However, the mechanisms by which TMS alleviates neuropathic pain, especially neuropathic pain induced by SCI, remain unclear. Previous studies have found that local cortical stimulation through TMS can cause functional changes in distant brain regions[8], whether it has a regulatory effect on the spinal cord after SCI is still unknown. Since the spinal cord serves as the primary processing center for limb pain, the regulatory effect and mechanisms of TMS on the spinal cord are issues worth investigating.

Here, we used resting-state functional MRI to determine that early TMS treatment at 1 week after SCI, enhanced functional connectivity between the cortex and thalamus, and increased tight connectivity in multiple brain regions. Then, to explore the mechanisms by which TMS regulates the brain and spinal cord in SCI mice, we performed sequencing on the thalamus, hypothalamus, and spinal cord. We found that TMS may improve the plasticity of pain-related brain areas and reduce spinal cord inflammation by activating the HPA axis.

2. Results

2.1. TMS continuously attenuated neuropathic pain after SCI

The experimental flow chart is shown in Fig. 1A. After contusion, the hind limbs of the mice were completely paralyzed, and their weight decreased but gradually recovered over time (Fig. 1B–C and Supplementary Table 1). Mechanical allodynia of both the left and right hindlimbs, along with cold hyperalgesia (paw withdrawal frequency vs. baseline) and thermal hyperalgesia (paw withdrawal latency vs. baseline), occurred at 14 dpi (cutoffs vs. baseline), gradually worsened and was sustained until 42 dpi (Fig. 1D–G). There was no statistically significant difference between the left and right hindlimbs or between the Sham group and Sham + TMS group (Fig. 1D–G). These results indicated that spinal cord contusion induced significant neuropathic pain symptoms. After TMS intervention at 1week postinjury, mechanical allodynia of the left hindlimb was attenuated from 28 dpi and sustained until 42 dpi (Fig. 1D); the mechanical allodynia of the right hindlimb was attenuated from 21 dpi and sustained until 42 dpi (Fig. 1E). After TMS intervention at 2 weeks postinjury, the mechanical allodynia of both the left and right hindlimbs was attenuated from 35 dpi and sustained until 42 dpi (Fig. 1D–E). It was suggested that TMS intervention at 1week postinjury may have an earlier mechanical allodynia attenuation effect than that at 2 weeks. Importantly, TMS intervention at both 1 week and 2 weeks postinjury showed a cold hyperalgesia relief effect at 14 dpi that was sustained until 42 dpi (Fig. 1F). Instead, TMS intervention of both groups showed thermal hyperalgesia attenuation until 42 dpi (Fig. 1G). In total, TMS attenuated spinal cord contusion-induced neuropathic pain, including mechanical allodynia and cold and thermal hyperalgesia. These pain relief effects were a durative process. Additionally, TMS intervention at 1 week had pain relief advantages compared to TMS intervention at 2 weeks.

2.2. TMS enhanced the functional connectivity between the motor cortex and the thalamus

Through functional magnetic resonance imaging (fMRI), we further detected brain changes in functional connectivity after TMS intervention. We found that TMS improved the regional homogeneity abnormalities in the secondary motor cortex caused by neuropathic pain (Fig. 2A). The TMS treatment after SCI group showed significant decreases in regional homogeneity (ReHo) values in the secondary motor area during the resting state compared with the control group with SCI (Fig. 2A). We selected 7 regions of interest (Rois) in the brain related to pain as seed points (Fig. 2B). We found that the strength of the functional connectivity between the primary motor cortex (MOp) and the thalamus was significantly increased after TMS treatment (Fig. 2B). Our results reflected that when compared with the control group, the nodal efficiency in right primary somatosensory area, the nodal shortest path in left primary somatosensory area, the betweenness centrality in right nucleus of the lateral lemniscus, the nodal clustering coefficient in left primary somatosensory area, and nodal local efficiency in right superior vestibular nucleus, were also increased in the TMS treatment group (Fig. 2C–D). These findings indicated that TMS intervention not only enhanced the functional connectivity between the cortex and the thalamus but also increased the close connection of multiple brain regions.

2.3. TMS activated the hypothalamic pituitary adrenal (HPA) axis in brain

To further investigate the changes in the brain after TMS intervention, the thalamus and hypothalamus were harvested for RNA-seq analysis. There was a total of 1527 differentially expressed genes (DEGs) after TMS intervention at 1 week between the SCI group and the SCI + TMS (1 week) group, including 785 upregulated and 742 downregulated DEGs. The GO enrichment and KEGG pathway

analysis revealed that the abundance of DEGs were enriched in several biological processes and signaling pathways, among which the most dominant biological processes and pathways were neuropeptide signaling pathway and neuroactive ligand–receptor interaction (Fig. 3A). The heatmap revealed the DEGs in the pathway of neuroactive ligand–receptor interaction (Fig. 3B). GSEA also showed the activation of the above two biological processes or pathways (Fig. 3C–D). Similarly, TMS intervention at 2 weeks was also observed to activate the neuropeptide signaling pathway and neuroactive ligand–receptor interaction (Supplementary Figs. 1A–C). Furthermore, through RT–PCR, we identified that the transcript levels of genes were significantly increased, including *Prl, Hcrt, Cga, Prlh, Pmch, Gh,*

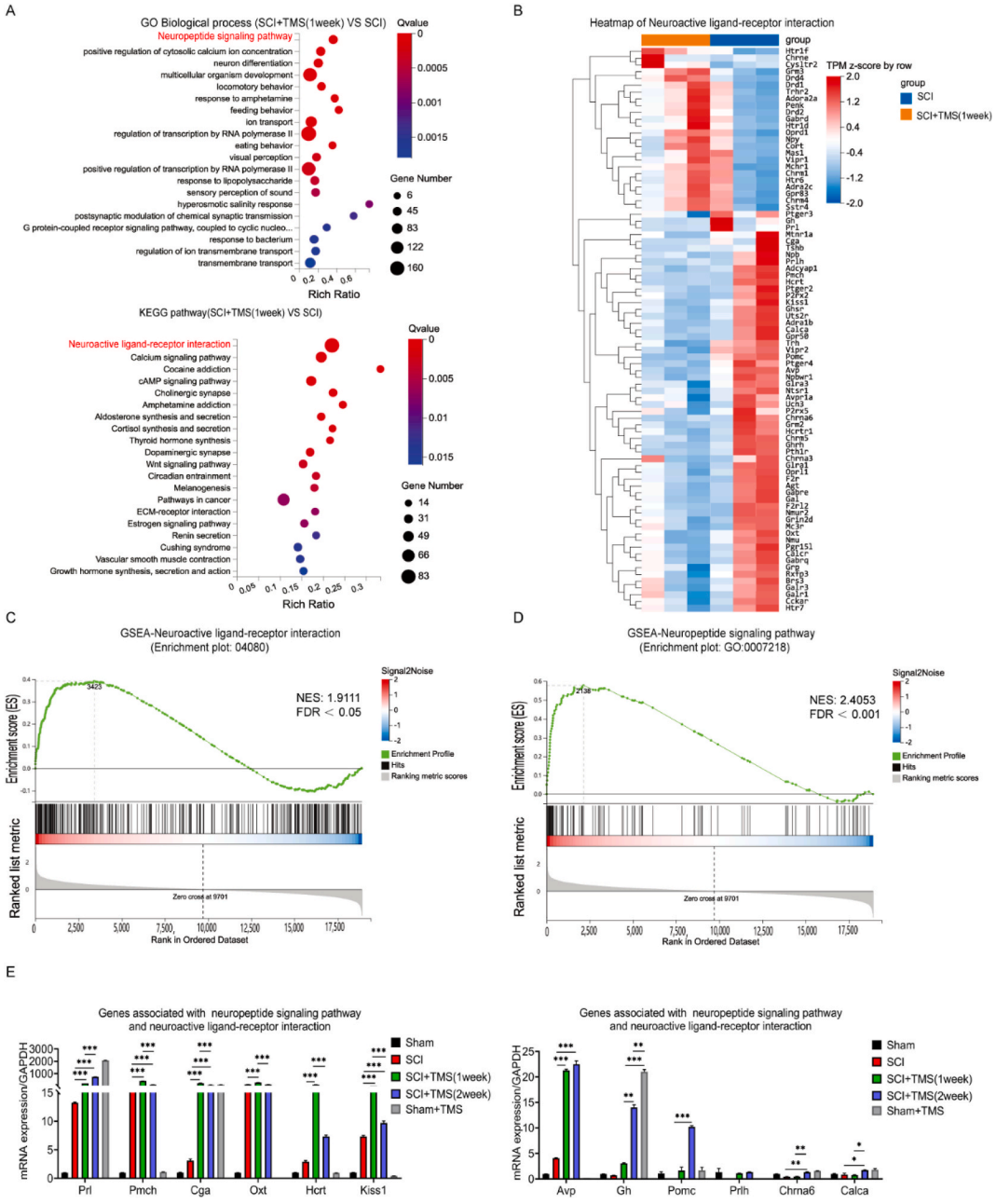

Fig. 3. TMS activated the hypothalamic pituitary adrenal (HPA) axis.
(**A**), GO enrichment and KEGG pathway analysis revealed the dominant biological process of DEGs and dysregulated signaling pathways in thalamus and hypothalamus between SCI group and SCI + TMS (1week) group. (**B**), the heatmap showed the DEGs between SCI group and SCI + TMS (1week) group. (**C-D**), GSEA analysis showed the dysregulated signaling pathways between SCI group and SCI + TMS (1week) group. (**E**), RT-PCR identified the effects of TMS treatment on mRNA expression of t neuropeptide signaling pathway and neuroactive ligand-receptor interaction. Values are the mean ± SEM. Statistical significance was determined by one-way ANOVA followed by Student Newman–Keuls post hoc test. n = 3 biological repeats. *P < 0.05, **P < 0.01, ***P < 0.001.

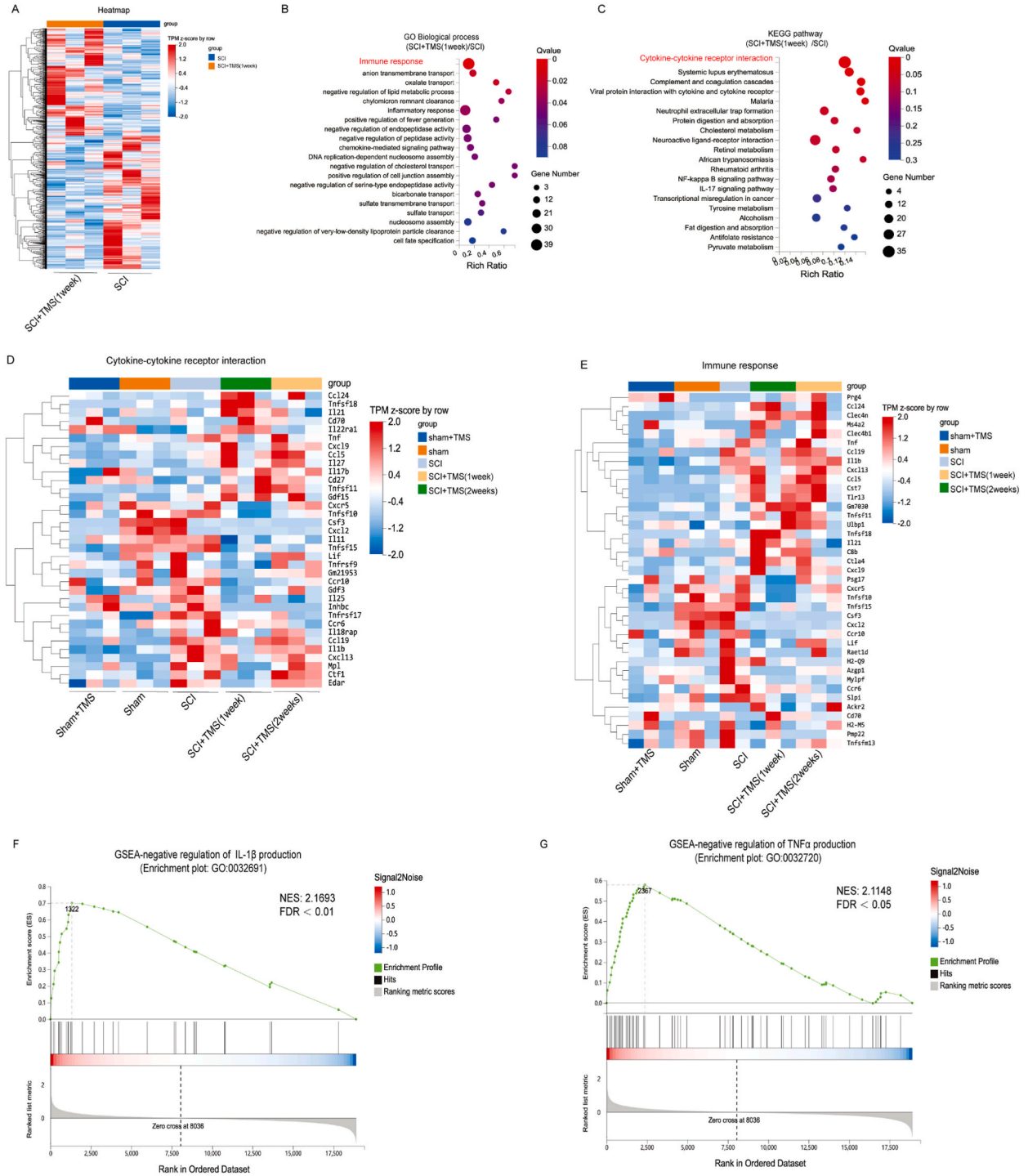

Fig. 4. TMS attenuated the local inflammatory microenvironment of spinal cord.
(**A**), the heatmap showed the DEGs between SCI group and SCI + TMS (1week) group in lumbar enlargement. (**B–C**), GO enrichment and KEGG pathway analysis revealed the dominant biological process of DEGs and dysregulated signaling pathways in lumbar enlargement between SCI group and SCI + TMS (1week) group. (**D-E**), The heatmaps showed the transcript level changes of these genes involved in immune response and cytokine-cytokine receptor interaction. (**F-G**), GSEA showed the activation of negative regulation of interleukin-1 beta (IL-1β) production and tumor necrosis factor (TNFα) production between SCI group and SCI + TMS (1week) group. n = 3 biological repeats.

Pomc, Chrna6, Avp, Oxt, Kiss1, and *Calca* (Fig. 3E), most of which encode hormone proteins that are involved in the HPA axis. Thus, as representatives of HPA axis function, their expression significantly increased after TMS intervention. These results indicated that TMS activated the HPA axis, which were closely associated with pain relief after SCI.

2.4. TMS attenuated the local inflammatory microenvironment in spinal cord

To further explore the potential mechanisms after TMS intervention, bulk RNA-seq was used to investigate the transcriptome changes in lumbar enlargement. The heatmap showed a total of 934 differentially expressed genes (DEGs) between the SCI group and the SCI + TMS (1 week) group, including 420 upregulated and 514 DEGs (Fig. 4A). The GO enrichment and KEGG pathway analysis revealed that the abundance of DEGs were enriched in several biological processes and signaling pathways, among which the most dominant biological processes and pathways were immune response and cytokine–cytokine receptor interaction (Fig. 4B–C). The heatmaps showed the transcript level changes of these genes involved in immune response and cytokine–cytokine receptor interaction (Fig. 4D–E). Moreover, GSEA showed the activation of the negative regulation of IL-1β production and TNFα production (Fig. 4F–G).

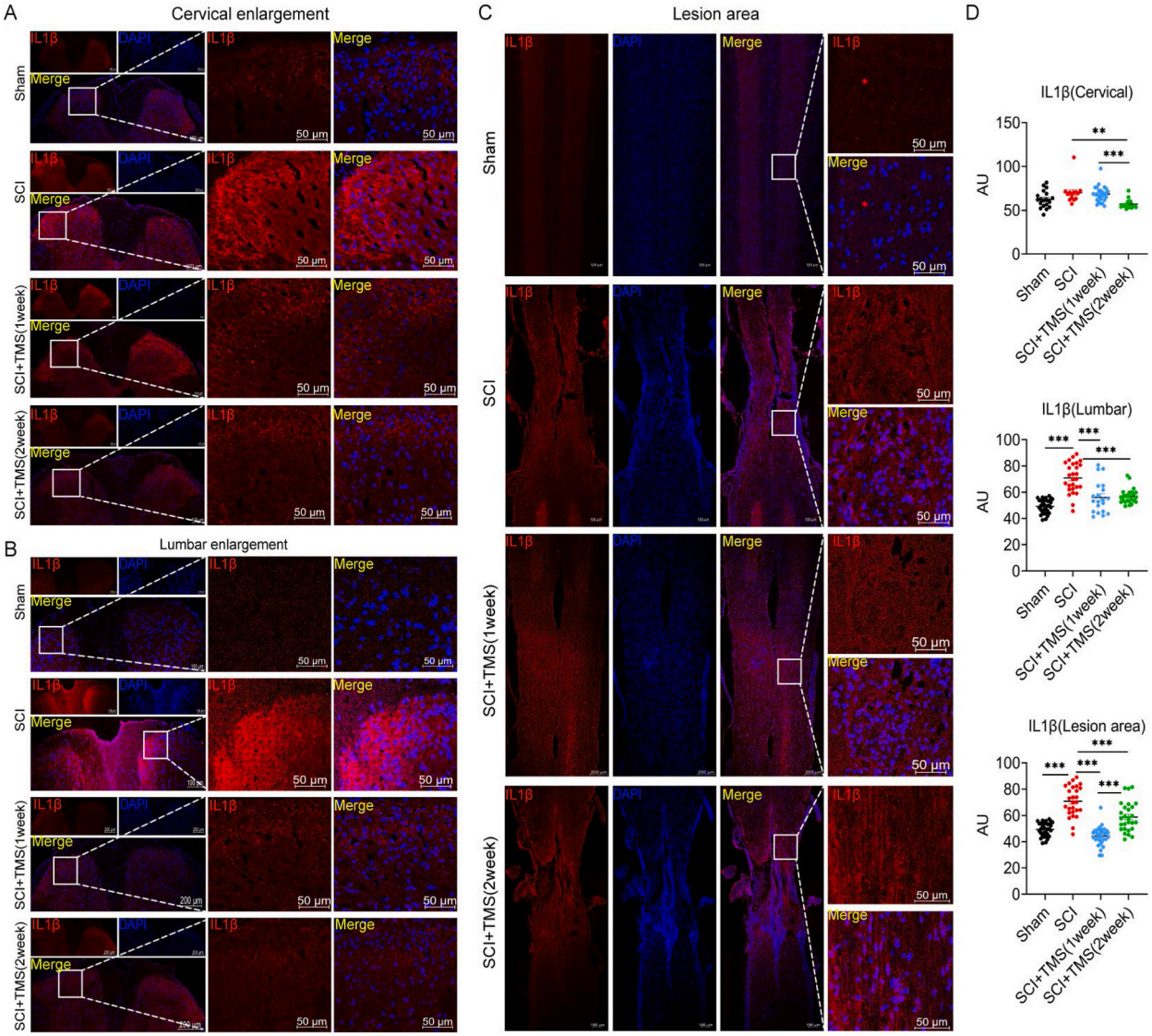

Fig. 5. TMS could significantly reduce the expression of IL-1β in lumbar enlargement, cervical enlargement and lesion area.
(**A**), images of immunofluorescent staining using IL-1β in cervical enlargement. Scale bar, 200 μm and 50 μm. n = 3 biological repeats. (**B**), images of immunofluorescent staining using IL-1β in lumbar enlargement. Scale bar, 200 μm and 50 μm. n = 3 biological repeats. (**C**), images of immunofluorescent staining using IL-1β in lesion area. Scale bar, 200 μm and 50 μm. n = 3 biological repeats. (**D**), statistical results of immunofluorescent staining. Values are the mean ± SEM. Statistical significance was determined by one-way ANOVA followed by Student Newman–Keuls post hoc test. n = 3 biological repeats. **P < 0.01, ***P < 0.001.

To further verify the RNA-seq results, lumbar enlargement tissues, along with tissues from cervical enlargement and lesion areas of the spinal cord, were obtained for immunofluorescence. We found that SCI induced significantly upregulated expression levels of IL-1β in the spinal cord, including lumbar enlargement, cervical enlargement and lesion areas (Fig. 5). TMS intervention at both 1 and 2 weeks could significantly reduce the expression of IL-1β in lumbar enlargement, cervical enlargement and lesion areas (Fig. 5A–D). Moreover, the expression of TNFα was downregulated in cervical enlargement and lumbar enlargement areas but not in lesion areas (Fig. 6A–D). Instead, the activation of microglia was not changed in cervical enlargement areas, increased in lumbar enlargement areas and inhibited in lesion areas (Fig. 6A–D). We found that TMS intervention at 1 week could significantly increase IL-10 expression (anti-inflammatory) and decrease macrophage activation (CD68) in cervical enlargement areas (Fig. 7A). Moreover, TMS intervention at 2 weeks could also increase IL-10 expression and decrease the activation of macrophages in lumbar enlargement areas (Fig. 7B). In lesion

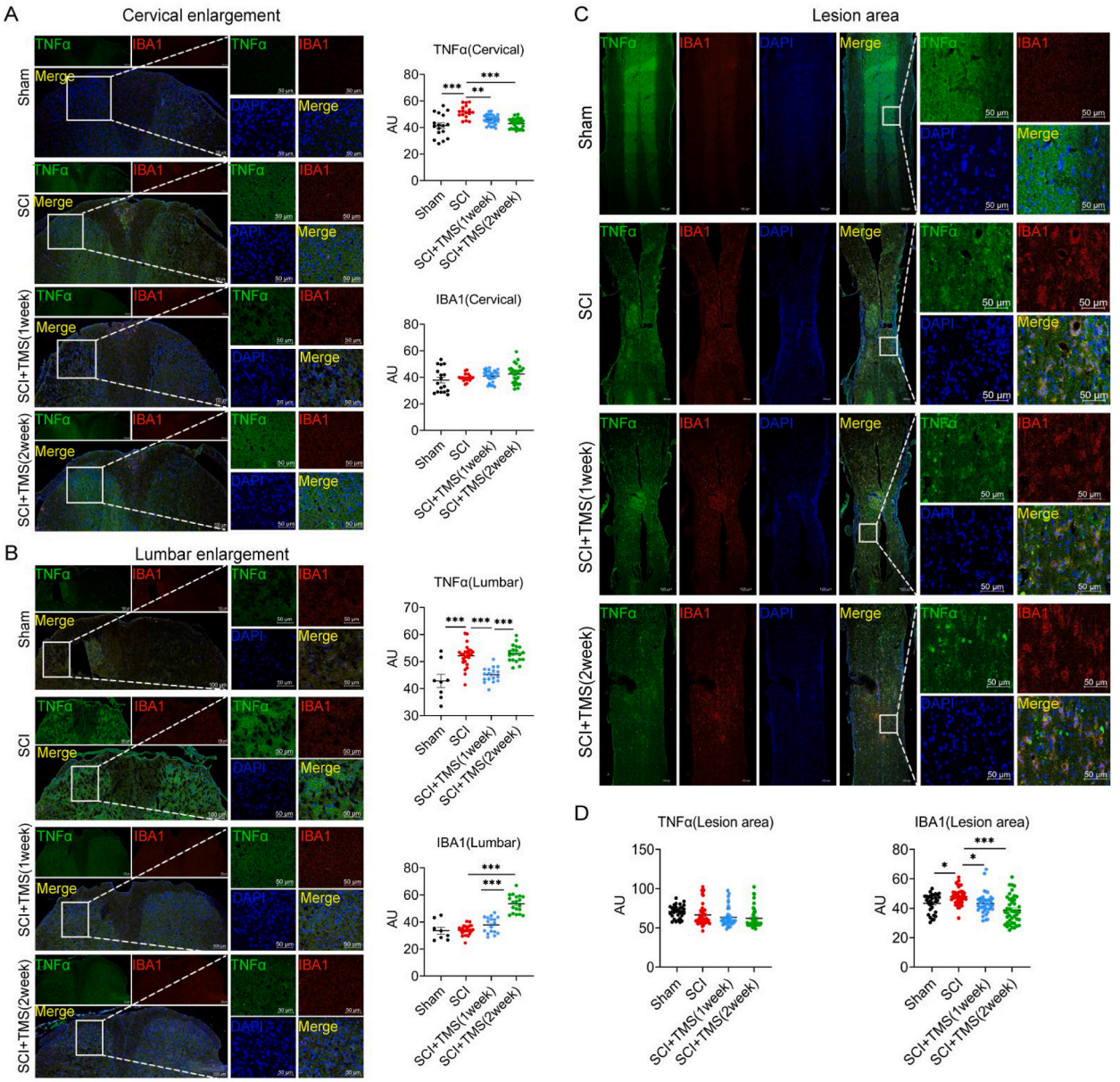

Fig. 6. TMS could significantly reduce the expression of TNFα in lumbar enlargement and cervical enlargement.
(**A**), images of immunofluorescent staining and statistical results using TNFα in cervical enlargement. Scale bar, 200 μm and 50 μm. n = 3 biological repeats. (**B**), images of immunofluorescent staining and statistical results using TNFα in lumbar enlargement. Scale bar, 200 μm and 50 μm. n = 3 biological repeats. (**C**), images of immunofluorescent staining and statistical results using TNFα in lesion area. Scale bar, 200 μm and 50 μm. n = 3 biological repeats. (**D**), statistical results of immunofluorescent staining. Values are the mean ± SEM. Statistical significance was determined by one-way ANOVA followed by Student Newman–Keuls post hoc test. n = 3 biological repeats. $^{**}P < 0.01$, $^{***}P < 0.001$.

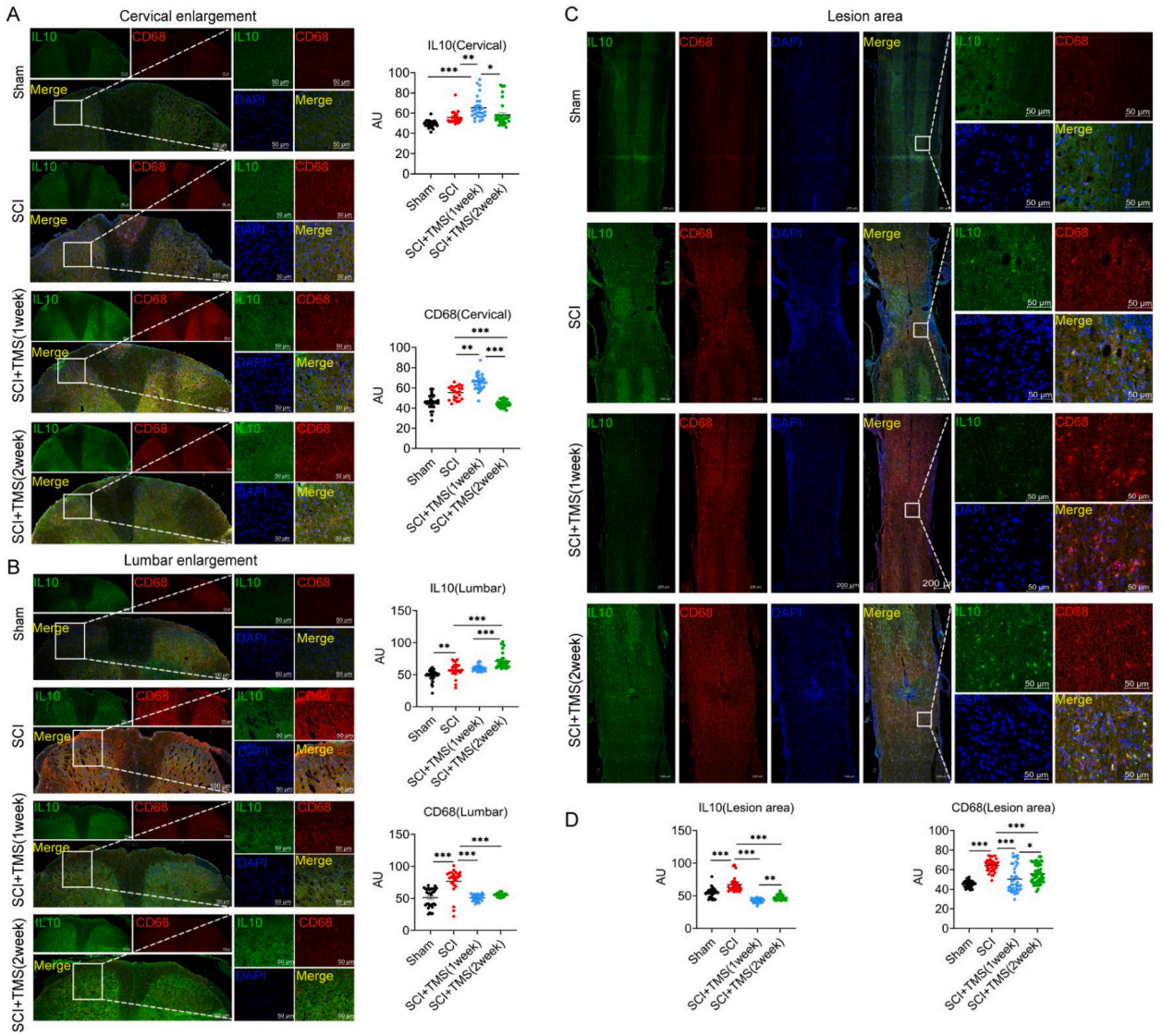

Fig. 7. TMS increased the IL-10 expression (anti-inflammatory) and decreased macrophages (CD68) activation in lumbar enlargement. (**A**), images of immunofluorescent staining and statistical results using IL-10 and CD68 in cervical enlargement. Scale bar, 200 μm and 50 μm. n = 3 biological repeats. (**B**), images of immunofluorescent staining and statistical results using IL-10 and CD68 in lumbar enlargement. Scale bar, 200 μm and 50 μm. n = 3 biological repeats. (**C-D**), images of immunofluorescent staining and statistical results using IL-10 and CD68 in lesion area. Scale bar, 200 μm and 50 μm. n = 3 biological repeats. Values are the mean ± SEM. Statistical significance was determined by one-way ANOVA followed by Student Newman–Keuls post hoc test. n = 3 biological repeats. *P < 0.05, **P < 0.01, ***P < 0.001.

areas, SCI induced a significant increase in IL-10 expression and macrophage activation (Fig. 7C–D). In contrast, TMS intervention inhibited the expression of IL-10 and macrophage activation (CD68) in lesion areas (Fig. 7C–D). Taken together, these results indicated that TMS attenuated the local inflammatory microenvironment in the spinal cord, which were closely associated with the improvement in neuropathic pain after SCI.

3. Discussion

In this study, we found that TMS could improve neuropathic pain after SCI. We determined the optimal time and intensity of TMS intervention, and further confirmed that TMS affected the functional connectivity of the brain, activated the HPA axis and further attenuated the inflammatory microenvironment in the spinal cord (Fig. 8). These changes were closely related to the improvement in neuropathic pain after SCI.

The optimal timepoint of TMS treatment for neuropathic pain was not yet clear. A recent study has summarized the role of TMS in improving the neuropathic pain induced by SCI and other conditions, along with the frequency and duration of TMS intervention [5].

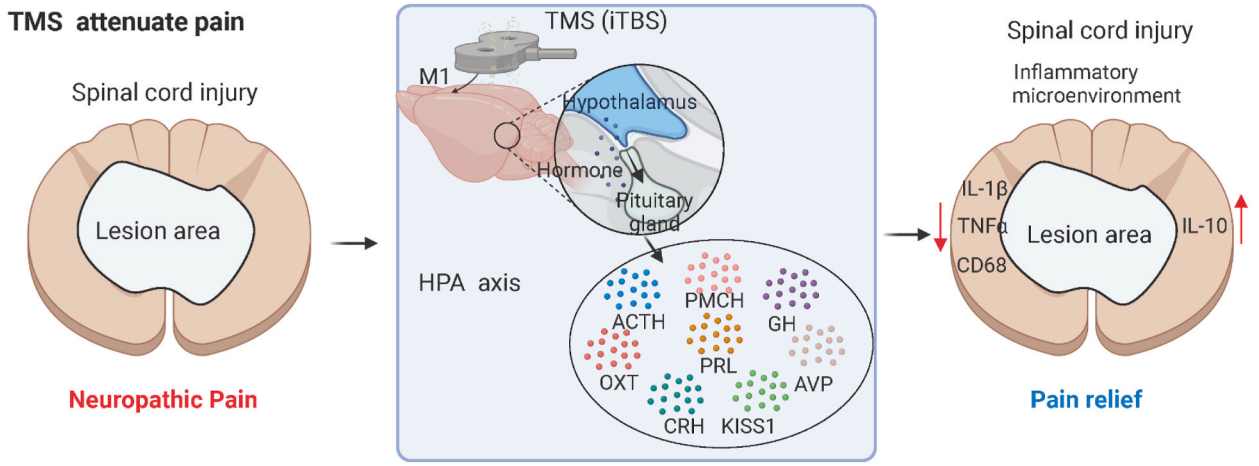

Fig. 8. The schematic diagram of this study (Created with BioRender.com).
TMS improved SCI-induced neuropathic pain. TMS treatment activated the hypothalamic pituitary adrenal (HPA) axis and increased the transcript levels of genes encode hormone proteins, which further attenuated the local inflammatory microenvironment in spinal cord associated with pain relief.

Generally, the M1 area, high-frequency with 5, 10 or 20 Hz, 80 %~90 % RMT and continuous stimulation for 5–21 days are currently the main parameters of TMS and would obtain a sustained pain improvement effect [5]. Thus, TMS intervention may bring about sustained improvement in neuropathic pain. Our findings revealed that high-frequency TMS reduced neuropathic pain after SCI, including mechanical allodynia and cold and thermal hyperalgesia. As previously reported[5], we found these pain-relieving effects are sustained. Furthermore, TMS intervention at 1 week appeared to be more beneficial for pain relief than at 2 weeks after SCI. We speculated that TMS may prevent pain before the pain circuit is established, which needs more clinical evidence or verification in more pain models to clarify whether early intervention with TMS may bring about pain improvement benefits to patients.

Long-term neuropathic pain may also affect the integrity of central autonomic neural networks through strong interactions of nociceptive and autonomic pathways in the spinal cord and brain [11,12], leading to neuroplastic changes in the hypothalamus, insula, anterior cingulate cortex and amygdala [13]. The thalamus and hypothalamus are key regions in regulating nociceptive and autonomic responses [11]. Our fMRI results revealed that TMS intervention enhanced the functional connectivity between the primary motor cortex and the thalamus. And by calculating the graph theory properties of the functional connectivity between pain-related brain regions, we found that compared to the sham intervention group, mice in the TMS intervention group exhibited: higher nodal efficiency, clustering coefficient, and shortest path length in the primary sensory cortex, higher local efficiency in the medulla (right superior vestibular nucleus), and higher betweenness centrality in the pons (right lateral lemniscus nucleus). This suggests that TMS intervention improved the working efficiency of pain-related brain regions in the structural network. A recent study found that painful diabetic neuropathy reduced the structural connectivity in several brain areas, including the thalamic nucleus in the limbic system, the thalamus and hypothalamus involving the amygdala and anterior cingulate cortex, and the structural connectivity between the hypothalamus and the infundibular subunit of the amygdala, which are associated with the severity of neuropathic pain [11]. These findings suggest that neuropathic pain has a negative impact on the hypothalamic limbic pathway [11]. Therefore, to some extent, TMS attenuated neuropathic pain after SCI, which may directly impact on brain function.

Another new finding is TMS activated the HPA axis. Previous study has summarized that SCI activates the HPA axis, which regulates glucocorticoid production, neuroinflammation, and neuropathic pain after SCI [14]. We found that the transcript levels of genes were significantly increased after TMS treatment, including *Prl, Hcrt, Cga, Prlh, Pmch, Gh, Pomc, Chrna6, Avp, Oxt, Kiss1,* and *Calca,* most of them encode hormone proteins are involved in the HPA axis. Among which, corticotropin-releasing hormone (CRH), encoded by the *Hcrt* gene, is a peptide hormone synthesized by the hypothalamus, and adrenocorticotropic hormone (ACTH), encoded by the *Cga* gene, is a hormone that is secreted by the pituitary gland. The *Oxt* gene encodes oxytocin (OXT), a peptide hormone synthesized by the hypothalamus that has been widely demonstrated to be involved in pain regulation [15–17]. Oxytocin neurons not only release oxytocin directly through axons to sensory spinal cord neurons and inhibit their activity, but also indirectly modulate peripheral nociception by stimulating supraoptic nucleus neurons to release oxytocin to sensory spinal cord neurons [15]. Importantly, oxytocin may also increase prelimbic prefrontal cortex responses to nociception by altering the local excitatory-inhibitory balance, and locally applied oxytocin may directly stimulate hypothalamic paraventricular nucleus neuron axon terminals to relieve pain through the prelimbic prefrontal cortex [17]. Furthermore, oxytocin in the anterior cingulate cortex attenuates neuropathic pain by inhibiting presynaptic long-term potentiation [16]. Thus, TMS treatment improves neuropathic pain may be through activating the HPA axis.

We also found that TMS intervention can attenuate the inflammatory environment in the spinal cord. Inflammatory cytokines can modulate inhibitory and excitatory synaptic transmission, ultimately improving the transmission of pain signals to the brain [5]. Conversely, neuropathic pain could induce persistent inflammation in the cortical area and spinal cord and further lead to persistent pain [5,18,19]. TMS treatment acts on the primary motor cortex (M1) area to reduce neuroinflammation, inhibit the activation of

astrocytes and microglia, and has analgesic effects, especially in SCI-induced pain [5]. At present, the mechanisms by which TMS treatment regulate the inflammatory environment in the spinal cord is not completely clear. The HPA axis is part of the limbic system of the brain and is responsible for the stress responses activated by pro-inflammatory cytokines [20]. In response to stress triggers, the HPA axis stimulates the hypothalamus to secrete CRF, which in turn stimulates the pituitary gland to secrete ACTH, ultimately leading to the release of cortisol from the adrenal glands [21]. Thus, the inflammatory microenvironment in spinal cord may be regulated by TMS induced HPA axis activation. Our study suggested that the mechanism by which HF-rTMS alleviates neuropathic pain after SCI may be the activation of the HPA axis in the brain, thereby controlling spinal cord inflammation. Further research is needed to explore the pathways through which the TMS-activated HPA axis in the brain remotely regulates the inflammatory environment of the spinal cord.The mechanisms underlying the development of neuropathic pain after SCI are complex, involving the interruption of descending inhibitory pain pathways post-SCI, leading to a series of pathological changes throughout the entire neural axis, including the brain cortex, thalamus, and spinal cord. Our study aims to explore the mechanisms by which TMS improves neuropathic pain after SCI. Therefore, we firstly used resting-state functional MRI to study the changes in brain functional connectivity after TMS intervention, to identify the brain target areas affected by TMS stimulation of the M1 region. We also performed RNA sequencing analysis on the brain's target areas—the thalamus and hypothalamus—to explore the regulatory mechanisms of TMS on the brain. RNA sequencing and RT-PCR experiments revealed that, compared to the control group, the transcription levels of genes encoding hormone proteins involved in the HPA axis were significantly increased in the brains of mice in the TMS intervention group, suggesting that TMS may exert its effects by activating the HPA axis in the brains of SCI mice. Since the spinal cord serves as the primary processing center for limb pain, it is highly likely that the mechanism by which TMS alleviates neuropathic pain after SCI also includes the remote regulatory effect of TMS on the spinal cord. We further conducted RNA sequencing of the spinal cord and found that, compared to the control group, the inflammatory response in the spinal cords of mice in the TMS intervention group was significantly improved. This was further confirmed through immunofluorescence staining of tissue sections.

The activation of the HPA axis can promote an increase in glucocorticoid secretion, and glucocorticoids can mitigate the excessive inflammatory response within the spinal cord caused by spinal cord injury, thereby protecting spinal neurons and glial cells. Based on our experimental results, we preliminarily propose our scientific hypothesis: the mechanism by which TMS alleviates neuropathic pain after spinal cord injury may involve the activation of the HPA axis to attenuate spinal cord inflammation.

4. Conculsion

Overall, early high-frequency TMS treatment could improve neuropathic pain after SCI associated with enhancing brain functional connectivity and HPA axis activity, which may further attenuate the inflammatory microenvironment in spinal cord. This preclinical animal study suggests that the application of TMS should be considered in the treatment of neuropathic pain after SCI, and the improvement in pain symptoms brought about by this noninvasive intervention is multifaceted.

5. Limitations of study

There are also some limitations. We did not further verify HPA axis activation in the brain or blood instead by RNA sequencing and RT-PCR. Although we determined that the TMS could significantly enhance brain functional connectivity and HPA axis activity, we did not further verify them through HPA axis intervention and other rescue experiments. Instead, we provided a strategy to potentially target and activate HPA axis activity to improve pain after SCI via TMS treatment. There is also a lack of more general observation of HPA axis activation in other pain models.

STAR★Methods

Resource availability

Lead contact

Further information and requests for resources and reagents should be directed to and will be fulfilled by the corresponding author, Prof. Ning Xie (nxieprof18@tongji.edu.cn).

Materials availability

This study did not generate new unique reagents.

Date and code availability

- Raw data and processed data of RNA-seq datasets generated during this study have been deposited in NCBI database under Sequence Read Archive (SRA) with Bioproject identification number PRJNA1063907 (https://dataview.ncbi.nlm.nih.gov/object/PRJNA1063907).
- This paper does not report original code.
- Any additional information required to reanalyze the data reported in this paper is available from the Lead Contact upon request.

Material and method details

Animals

All procedures were carried out in accordance with the U.K. Animals (Scientific Procedures) Act, 1986 and associated guidelines, EU Directive 2010/63/EU for animal experiments, and approved by the Institutional Animal Care and Use Committee (IACUC) of Tongji University School of Medicine (No. 2021-DW - (010), 2021-05-06). The experimental program aims to minimize the number of animals used and the suffering of animals. C57/BL6 female mice were obtained from Shanghai Jiesijie Laboratory Animal Co., Ltd. Mice are raised in a 12/12-h light/dark cycle and can freely obtain food and water. This study only investigated female mice for the previous findings revealed the sex-dependent difference in neuropathic pain after SCI [22,23]. The room temperature and humidity were appropriate. All behavioral tests are conducted between 9:00 a.m. and 5:00 p.m. A total of 60 C57/BL6 female mice aged 2 months were randomly divided into the following groups: sham group, n = 10; sham + TMS group, n = 5; SCI group, n = 15; SCI + TMS (1week) group, n = 15; SCI + TMS (2week) group, n = 15. SCI + TMS (1week) group and SCI + TMS (2week) group represented TMS treatment at 1 week and 2 weeks after SCI, respectively.

Spinal cord contusion model and motor function test

Thoracic spinal cord contusion is a widely used SCI model for neuropathic pain [24], and the MASCIS Impactor Model III (W.M. Keck Center for Collaborative Neuroscience, Rutgers, the State University of New Jersey, USA) were applied as we previously reported [25,26]. Briefly, a laminectomy at T10 was performed through an operating microscope (Zeiss, Germany) and rodent stereotaxic apparatus (RWD Life Science Co.,Ltd, Shenzhen, China). Contusion was performed at T10 with a 5 g impactor and 6.25 mm height with a force of about 60 kdyn, a moderate injury as we previously reported [25]. Mice had received natural illumination to keep warm during the surgery. Sham mice underwent laminectomy but not contusion. Urine was manually expressed from the bladders of the injured mice twice per day. Hindlimb motor function was tested in an open field chamber on days 0, 1 and 3 after SCI and weekly for up to 6 weeks. The Basso Mouse Scale (BMS) [27] was applied to quantify motor function by two investigators blinded to the group assignments.

Mechanical sensitivity measurement

Pain test was applied as we previously reported [25] and described in the experimental flow chart (Fig. 1A). The electronic Von-Frey apparatus (IITC Life Sciences, Woodland Hills, CA) was used to measure the mechanical allodynia of the hindlimbs [25]. Behaviours that were considered positive responses to the filament included brisk paw withdrawal, flinching, hunching of the back, licking of the stimulated area, and escape responses [25]. All animals underwent 2 trials (5 measurements/trial) at 24 and 48 h before contusion to calculate the average plantar paw withdrawal threshold of both hindlimbs at baseline. The measurement was performed in a blinded fashion at 14 days post injury (dpi), 21dpi, 28dpi, 35dpi, and 42dpi after spinal cord contusion.

Analgesia test for cold and thermal pain

Cold and hot plate (Cat# YSL-21; Shanghai Yuyan Instruments Co., Ltd. China) was used to assess cold and thermal pain as we previously reported [25]. The temperatures of 0 °C (cold stimulus) and 50 °C (hot stimulus) were used to measure the thresholds for noxious heat and cold, respectively [25]. The positive response included licking, jumping or hind paw withdrawal. For hot stimuli, the paw withdrawal latency was recorded and means the period from touching the hot plate to the emergence of positive response. For cold stimuli, the paw withdrawal frequency was recorded and means the number of nociceptive responses observed in 5 min on cold plate. The process was carried out as mechanical allodynia test and described in the experimental flow chart (Fig. 1A). The tests were conducted by two investigators blinded to the groups and experimental conditions.

Intermittent theta-burst stimulation (iTBS)

The intermittent theta burst stimulation (iTBS) is a form of repetitive TMS and is associated with a significant decrease in neuropathic pain [28,29]. iTBS treatment was described in the experimental flow chart (Fig. 1A). To avoid the impact of repeated anesthesia on mouse brain function, iTBS was performed in a conscious state without anesthesia or sedation. The operator fixes the bilateral shoulder joints of the mice with their hands. Then, we placed the stimulation coils (MC-B35, MagVenture Co.) of the magnetic stimulator (MagPro X100, MagVenture Co., Farum, Denmark) in the motor cortex area (M1) of the skull. Firstly, according to standard practice, the Active Motion Threshold (AMT) was determined through visual observation. Then, a 50 Hz pulse triple recombination, at 80 % AMT (40 % of the maximum output intensity of the machine), was applied 2s on and 8s off at 5 Hz, repeated 20 times, and generated 600 total pulses with a total duration of 3 min and 9s [30]. The sham + TMS group also received the same iTBS stimulation, but the coil was perpendicular to the scalp. Throughout the entire stimulation process, all groups of mice were able to quietly cooperate with the stimulation, without any obvious side effects. SCI + TMS (1week) group received transcranial iTBS at 1 week post injury and SCI + TMS (2week) group were at 2 weeks. Transcranial iTBS was carried out once a day and continuously for 5 days per week until 42 dpi. The TMS treatment began at 1 week for the overall condition of the mice were stable and had gradually recovered from the contusion injury.

Functional magnetic resonance imaging (fMRI) acquisition and analysis

Mice in the TMS group (SCI with TMS treatment, n = 6) and control group (SCI without TMS treatment, n = 6) performed MRI examination on 42 dpi. Resting-state fMRI was carried out in a dedicated small-animal 7.0-T MRI system (BioSpec 70/20 Ultra Shielded and Re-frigerated, Bruker) using a 1H quadrature transmit/receive surface coil with a 112/86 mm inner diamet. The mice were anesthetized with isoflurane, and the respiration was continuously monitored during all fMRI experiments. Standard adjustments included the calibration of the reference frequency power and the shim gradients using MapShim (ParaVision 6.0.1). To construct a reference for the brain anatomy, high-resolution T2-weighted images (T2WIs) of the whole brain were acquired using a Rapid Acquisition with Relaxation Enhancement (RARE) method with the following parameters: effective time to echo (TE) = 36 ms, time to repetition (TR) = 3000 ms, RARE factor = 8, number of averages = 2, and number of slices = 25. The BOLD fMRI signal was acquired using a gradient echo-echo planar imaging method with the following parameters: TE = 19.6 ms, TR = 2000 ms, number of averages = 1, number of slices = 16, and slice thickness = 0.5 mm. The scan was repeated 300 times in 10 min. The fMRI data analysis was described in **Additional file** (Appendix 1).

RNA sequencing (RNA-seq) and bioinformatics analysis

Thalamus and hypothalamus are key regions that regulate nociceptive and autonomic responses [11]. The ascending tracts and superficial dorsal horn (SDH) in lumbar enlargement are closely associated with proprioception and pain signal processing of the lower limbs [31]. Thus, brain tissues (the thalamus and hypothalamus) and spinal cord tissues (the lumbar enlargement) of mice were obtained for RNA-seq experiment to further evaluate the role of iTBS in gene expression regulation and pain attenuation mechanisms, including sham group (spinal cord, n = 3; brain, n = 3), sham + TMS group (spinal cord, n = 3; brain, n = 3), SCI group (spinal cord, n = 3; brain, n = 3), SCI + TMS (1week) group (spinal cord, n = 3; brain, n = 3) and SCI + TMS (2week) group (spinal cord, n = 3; brain, n = 3). The detailed description of the RNA-seq and data analysis is available in Supplementary Materials (Appendix 2). Raw data and processed data of RNA-seq datasets generated during this study have been deposited in NCBI database under Sequence Read Archive (SRA) with Bioproject identification number PRJNA1063907 (https://dataview.ncbi.nlm.nih.gov/object/PRJNA1063907).

Quantitative real-time PCR (RT–PCR)

The total RNA of cells was isolated with RNAiso plus (Cat# 9108, Takara). The concentration and purity of RNA samples were measured using a Nanodrop ND-2000 (Thermo Science, MA, USA) for further experiments. Five hundred nanograms of RNA was converted to complementary DNA (cDNA), which was synthesized with a PrimeScript reverse transcriptase kit (Cat# RR037A, Takara). RT–PCR was performed using a TB Green TM Premix Ex Taq Kit (Cat# RR820A, Takara) on a Light Cycler Real-Time PCR System (480II, Roche). The primer sequences (Shanghai Generay Biotech Co., Ltd.) were designed through PrimerBank (https://pga.mgh.harvard.edu/primerbank/) and are listed in Supplementary Table 2. The relative amounts of mRNA were calculated using the ΔΔCt relative quantification method. GAPDH served as the control gene, and the mRNA levels of specific genes were normalized to GAPDH. Calculations and statistics were performed in Microsoft Excel version 16.36. Graphs were plotted in GraphPad Prism 8 version 8.4.3.

Immunofluorescence staining and analysis

Immunofluorescence staining procedures and analysis were conducted as we previously described [26]. The primary antibodies used were as follows: Ionized calcium binding adaptor molecule 1 (IBA1, Cat# 016–20001, Wako, 1:500), CD68 (Cat#28058-1-AP, Peprotech, 1:100), IL-10 (Cat#60269-1, Peprotech, 1:100), IL-1β (Cat#16806-1-AP, Peprotech, 1:100), TNF-α (Cat# ab1793, Abcam, 1:200). The secondary antibodies were Alexa® Fluor 488 (Cat# abs20019A, Absin, 1:500), Alexa® Fluor 488 (Cat# A-32766, Invitrogen, 1:500), Alexa Fluor®488 (Cat#706-545-148, Jackson, 1:100), Alexa Fluor® 555 (Cat# A-32794, invitrogen, 1:200), Alexa Fluor® 647 (Cat# 703-605-155, Jackson, 1:200). The nuclei were stained with 4′,6-diamidino-2-phenylindole (DAPI, Cat# C1002, Beyotime Institute of Biotechnology), and fluorescence images were taken and assembled as we previously described [26]. For Sham group and treatment groups, three mice per group were tested.

Quantification and statistical analysis

Statistical analysis

All continuous data were shown as mean ± SEM. ANOVA was performed followed by Student Newman-Keuls post hoc test for continuous data. Statistical analysis was carried out in SAS 9.3 (SAS Institute, Inc., Cary, NC, USA). Two-sided P values < 0. 05 were considered statistically significant. Plots were generated using GraphPad Prism 8 software (version 8.4.3, GraphPad Software, San Diego, CA).

Key resources table

REAGENT or RESOURCE	SOURCE	IDENTIFIER
Antibodies		
IBA1	Wako	Cat# 016-20001
CD68	Peprotech	Cat#28058-1-AP
IL-10	Peprotech	Cat#60269-1
IL-1β	Peprotech	Cat#16806-1-AP
TNF-α	Abcam	Cat# ab1793
Alexa® Fluor 488	Absin	Cat# abs20019A
Alexa® Fluor 488	Invitrogen	Cat# A-32766
Alexa Fluor®488	Jackson	Cat#706-545-148
Alexa Fluor® 555	invitrogen	Cat# A-32794
Alexa Fluor® 647	Jackson	Cat# 703-605-155
DAPI	Beyotime Institute of Biotechnology	Cat# C1002
Deposited data		
Raw data and processed data of RNA-seq datasets	Sequence Read Archive (SRA)	https://dataview.ncbi.nlm.nih.gov/object/PRJNA1063907
Experimental models		
Mouse:C57BL/6J wild type	Shanghai Jiesijie Laboratory Animal Co., Ltd	N/A
Oligonucleotides(mouse)		
Primer: Cga_F *CAAGCTAGGAGCCCCCATCTA*	Shanghai Generay Biotech Co., Ltd.	http://www.generay.com.cn/
Primer: Cga_R *CACTCTGGCATTTCCCATTACT*	Shanghai Generay Biotech Co., Ltd.	http://www.generay.com.cn/
Primer: Prl_F *CAGGGGTCAGCCCAGAAAG*	Shanghai Generay Biotech Co., Ltd.	http://www.generay.com.cn/
Primer: Prl_R *TCACCAGCGGAACAGATTGG*	Shanghai Generay Biotech Co., Ltd.	http://www.generay.com.cn/
Primer: Hcrt_F *GTCGCCAGAAGACGTGTTC*	Shanghai Generay Biotech Co., Ltd.	http://www.generay.com.cn/
Primer: Hcrt_R *GGTGGTAGTTACGGTCGGAC*	Shanghai Generay Biotech Co., Ltd.	http://www.generay.com.cn/
Primer: Pmch_F *GTCTGGCTGTAAAACCTTACCTC*	Shanghai Generay Biotech Co., Ltd.	http://www.generay.com.cn/
Primer: Pmch_R *CCTGAGCATGTCAAAATCTCTCC*	Shanghai Generay Biotech Co., Ltd.	http://www.generay.com.cn/
Primer: Prlh_F *TGCTGCTGCTAGGCTTAGTC*	Shanghai Generay Biotech Co., Ltd.	http://www.generay.com.cn/
Primer: Prlh_R *CGTGTACCAGGCAGGATTGA*	Shanghai Generay Biotech Co., Ltd.	http://www.generay.com.cn/
Primer: Gh_F *GCTACAGACTCTCGGACCTC*	Shanghai Generay Biotech Co., Ltd.	http://www.generay.com.cn/
Primer: Gh_R *CGGAGCACAGCATTAGAAAACAG*	Shanghai Generay Biotech Co., Ltd.	http://www.generay.com.cn/
Primer: Pomc_F *ATGCCGAGATTCTGCTACAGT*	Shanghai Generay Biotech Co., Ltd.	http://www.generay.com.cn/
Primer: Pomc_R *TCCAGCGAGAGGTCGAGTTT*	Shanghai Generay Biotech Co., Ltd.	http://www.generay.com.cn/
Primer: Avp_F *GCCAGGATGCTCAACACTACG*	Shanghai Generay Biotech Co., Ltd.	http://www.generay.com.cn/
Primer: Avp_R *TCTCAGCTCCATGTCAGAGATG*	Shanghai Generay Biotech Co., Ltd.	http://www.generay.com.cn/
Primer: Chrna6_F *TAAAGGCAGTACAGGCTGTGA*	Shanghai Generay Biotech Co., Ltd.	http://www.generay.com.cn/
Primer: Chrna6_R *AAAATGCACCGTGACGGGAT*	Shanghai Generay Biotech Co., Ltd.	http://www.generay.com.cn/
Primer: Oxt_F *CCGAAGCAGCGTCCTTT*	Shanghai Generay Biotech Co., Ltd.	http://www.generay.com.cn/
Primer: Oxt_R *CTTGGCTTACTGGCTCTGAC*	Shanghai Generay Biotech Co., Ltd.	http://www.generay.com.cn/
Primer: Calca_F *GAGGGCTCTAGCTTGGACAG*	Shanghai Generay Biotech Co., Ltd.	http://www.generay.com.cn/
Primer: Calca_R *AAGGTGTGAAACTTGTTGAGGT*	Shanghai Generay Biotech Co., Ltd.	http://www.generay.com.cn/
Primer: Kiss1_F *CTCCTCTGTGTCGCCACCTA*	Shanghai Generay Biotech Co., Ltd.	http://www.generay.com.cn/
Primer: Kiss1_R *TTCCCAGGCATTAACGAGTTC*	Shanghai Generay Biotech Co., Ltd.	http://www.generay.com.cn/
Primer: Gapdh_F *AGGTCGGTGTGAACGGATTTG*	Shanghai Generay Biotech Co., Ltd.	http://www.generay.com.cn/
Primer: Gapdh_R *TGTAGACCATGTAGTTGAGGTCA*	Shanghai Generay Biotech Co., Ltd.	http://www.generay.com.cn/

CRediT authorship contribution statement

Qing Zhao: Writing – review & editing, Writing – original draft, Visualization, Validation, Software, Resources, Methodology, Investigation, Funding acquisition, Formal analysis, Data curation, Conceptualization. **Lijuan Zhao:** Writing – review & editing, Writing – original draft, Visualization, Validation, Software, Resources, Methodology, Investigation, Formal analysis, Data curation, Conceptualization. **Pianpian Fan:** Writing – review & editing, Writing – original draft, Visualization, Supervision, Software, Project administration, Methodology, Investigation, Funding acquisition, Data curation, Conceptualization. **Yanjing Zhu:** Software, Resources, Methodology, Investigation. **Rongrong Zhu:** Writing – review & editing, Supervision, Funding acquisition, Data curation, Conceptualization. **Liming Cheng:** Writing – review & editing, Supervision, Resources, Project administration, Funding acquisition, Data curation, Conceptualization. **Ning Xie:** Writing – review & editing, Writing – original draft, Supervision, Project administration, Investigation, Funding acquisition, Data curation, Conceptualization.

Declaration of competing interest

The authors declare that they have no known competing financial interests or personal relationships that could have appeared to influence the work reported in this paper.

Acknowledgments

This work was supported by Shanghai Blue Cross Brain Hospital Co., Ltd. And Shanghai Tongji University Education Development Foundation, China; Programs in Emergency and Critical Care Medicine of Tongji Hospital, Tongji University, China (KPB1702); Tongji Hospital Supporting Funds, Tongji University, China (GJ2301); Shanghai Top Research Center Category B Project, China (2023ZZ02016); the National Natural Science Foundation of China, China (Grant Nos. 81974190); the Natural Science Foundation of Sichuan Province, China (No. 2023NSFSC1625); President Foundation of The Third Affiliated Hospital of Southern Medical University, China (No. YQ202308); Guangdong Basic and Applied Basic Research Foundation, China (No. 2023A1515110546).

Appendix A. Supplementary data

Supplementary data to this article can be found online at https://doi.org/10.1016/j.heliyon.2024.e36061.

References

[1] P. Henwood, J.A. Ellis, Chronic neuropathic pain in spinal cord injury: the patient's perspective, Pain Res. Manag. 9 (2004) 39–45, https://doi.org/10.1155/2004/863062.
[2] R.H. Dworkin, M. Backonja, M.C. Rowbotham, R.R. Allen, C.R. Argoff, G.J. Bennett, M.C. Bushnell, J.T. Farrar, B.S. Galer, J.A. Haythornthwaite, et al., Advances in neuropathic pain: diagnosis, mechanisms, and treatment recommendations, Arch. Neurol. 60 (2003) 1524–1534, https://doi.org/10.1001/archneur.60.11.1524.
[3] N. Attal, F. Poindessous-Jazat, E. De Chauvigny, C. Quesada, A. Mhalla, S.S. Ayache, C. Fermanian, J. Nizard, R. Peyron, J.P. Lefaucheur, D. Bouhassira, Repetitive transcranial magnetic stimulation for neuropathic pain: a randomized multicentre sham-controlled trial, Brain 144 (2021) 3328–3339, https://doi.org/10.1093/brain/awab208.
[4] H. Knotkova, C. Hamani, E. Sivanesan, M.F.E. Le Beuffe, J.Y. Moon, S.P. Cohen, M.A. Huntoon, Neuromodulation for chronic pain, Lancet (London, England) 397 (2021) 2111–2124, https://doi.org/10.1016/S0140-6736(21)00794-7.
[5] Y.W. Bai, Q.H. Yang, P.J. Chen, X.Q. Wang, Repetitive transcranial magnetic stimulation regulates neuroinflammation in neuropathic pain, Front. Immunol. 14 (2023) 1172293, https://doi.org/10.3389/fimmu.2023.1172293.
[6] K. Hosomi, T. Shimokawa, K. Ikoma, Y. Nakamura, K. Sugiyama, Y. Ugawa, T. Uozumi, T. Yamamoto, Y. Saitoh, Daily repetitive transcranial magnetic stimulation of primary motor cortex for neuropathic pain: a randomized, multicenter, double-blind, crossover, sham-controlled trial, Pain 154 (2013) 1065–1072, https://doi.org/10.1016/j.pain.2013.03.016.
[7] R.J. Leo, T. Latif, Repetitive transcranial magnetic stimulation (rTMS) in experimentally induced and chronic neuropathic pain: a review, J. Pain 8 (2007) 453–459, https://doi.org/10.1016/j.jpain.2007.01.009.
[8] X. Moisset, D.C. de Andrade, D. Bouhassira, From pulses to pain relief: an update on the mechanisms of rTMS-induced analgesic effects, Eur. J. Pain 20 (2016) 689–700, https://doi.org/10.1002/ejp.811.
[9] R. Cavaleri, L.S. Chipchase, S.J. Summers, S.M. Schabrun, Repetitive transcranial magnetic stimulation of the primary motor cortex expedites recovery in the transition from acute to sustained experimental pain: a randomised, controlled study, Pain 160 (2019) 2624–2633, https://doi.org/10.1097/j.pain.0000000000001656.
[10] C. Quesada, B. Pommier, C. Fauchon, C. Bradley, C. Créac'h, M. Murat, F. Vassal, R. Peyron, New procedure of high-frequency repetitive transcranial magnetic stimulation for central neuropathic pain: a placebo-controlled randomized crossover study, Pain 161 (2020) 718–728, https://doi.org/10.1097/j.pain.0000000000001760.
[11] C.C. Chao, M.T. Tseng, P.C. Hsieh, C.J. Lin, S.L. Huang, S.T. Hsieh, M.C. Chiang, Brain mechanisms of pain and dysautonomia in diabetic neuropathy: connectivity changes in thalamus and hypothalamus, J. Clin. Endocrinol. Metabol. 107 (2022) e1167–e1180, https://doi.org/10.1210/clinem/dgab754.
[12] P. Cortelli, G. Giannini, V. Favoni, S. Cevoli, G. Pierangeli, Nociception and autonomic nervous system, Neurol. Sci. : official journal of the Italian Neurological Society and of the Italian Society of Clinical Neurophysiology 34 (Suppl 1) (2013) S41–S46, https://doi.org/10.1007/s10072-013-1391-z.
[13] A.S. Jaggi, N. Singh, Role of different brain areas in peripheral nerve injury-induced neuropathic pain, Brain Res. 1381 (2011) 187–201, https://doi.org/10.1016/j.brainres.2011.01.002.

[14] J.K. Lerch, D.A. Puga, O. Bloom, P.G. Popovich, Glucocorticoids and macrophage migration inhibitory factor (MIF) are neuroendocrine modulators of inflammation and neuropathic pain after spinal cord injury, Semin. Immunol. 26 (2014) 409–414, https://doi.org/10.1016/j.smim.2014.03.004.
[15] M. Eliava, M. Melchior, H.S. Knobloch-Bollmann, J. Wahis, M. da Silva Gouveia, Y. Tang, A.C. Ciobanu, R. Triana Del Rio, L.C. Roth, F. Althammer, et al., A new population of parvocellularoxytocin neurons controlling magnocellular neuron activity and inflammatory pain processing, Neuron 89 (2016) 1291–1304, https://doi.org/10.1016/j.neuron.2016.01.041.
[16] X.H. Li, T. Matsuura, M. Xue, Q.Y. Chen, R.H. Liu, J.S. Lu, W. Shi, K. Fan, Z. Zhou, Z. Miao, et al., Oxytocin in the anterior cingulate cortex attenuates neuropathic pain and emotional anxiety by inhibiting presynaptic long-term potentiation, Cell Rep. 36 (2021) 109411, https://doi.org/10.1016/j.celrep.2021.109411.
[17] Y. Liu, A. Li, C. Bair-Marshall, H. Xu, H.J. Jee, E. Zhu, M. Sun, Q. Zhang, A. Lefevre, Z.S. Chen, et al., Oxytocin promotes prefrontal population activity via the PVN-PFC pathway to regulate pain, Neuron 111 (2023) 1795–1811.e1797, https://doi.org/10.1016/j.neuron.2023.03.014.
[18] J. Li, G.H. Wei, H. Huang, Y.P. Lan, B. Liu, H. Liu, W. Zhang, Y.X. Zuo, Nerve injury-related autoimmunity activation leads to chronic inflammation and chronic neuropathic pain, Anesthesiology 118 (2013) 416–429, https://doi.org/10.1097/ALN.0b013e31827d4b82.
[19] G.D. Silva, P.S. Lopes, E.T. Fonoff, R.L. Pagano, The spinal anti-inflammatory mechanism of motor cortex stimulation: cause of success and refractoriness in neuropathic pain? J. Neuroinflammation 12 (2015) 10, https://doi.org/10.1186/s12974-014-0216-1.
[20] M. Carabotti, A. Scirocco, M.A. Maselli, C. Severi, The gut-brain axis: interactions between enteric microbiota, central and enteric nervous systems, Ann. Gastroenterol. 28 (2015) 203–209.
[21] O. Karin, M. Raz, A. Tendler, A. Bar, Y. Korem Kohanim, T. Milo, U. Alon, A new model for the HPA axis explains dysregulation of stress hormones on the timescale of weeks, Mol. Syst. Biol. 16 (2020) e9510, https://doi.org/10.15252/msb.20209510.
[22] N.T. Fiore, Z. Yin, D. Guneykaya, C.D. Gauthier, J.P. Hayes, A. D'Hary, O. Butovsky, G. Moalem-Taylor, Sex-specific transcriptome of spinal microglia in neuropathic pain due to peripheral nerve injury, Glia 70 (2022) 675–696, https://doi.org/10.1002/glia.24133.
[23] A.N. Stewart, J.L. Lowe, E.P. Glaser, C.A. Mott, R.K. Shahidehpour, K.E. McFarlane, W.M. Bailey, B. Zhang, J.C. Gensel, Acute inflammatory profiles differ with sex and age after spinal cord injury, J. Neuroinflammation 18 (2021) 113, https://doi.org/10.1186/s12974-021-02161-8.
[24] J.L. Kramer, N.K. Minhas, C.R. Jutzeler, E.L. Erskine, L.J. Liu, M.S. Ramer, Neuropathic pain following traumatic spinal cord injury: models, measurement, and mechanisms, J. Neurosci. Res. 95 (2017) 1295–1306, https://doi.org/10.1002/jnr.23881.
[25] Q. Zhao, L. Zhao, P. Fan, Y. Zhu, R. Zhu, L. Cheng, N. Xie, The positive correlation between motor function and neuropathic pain-like behaviors after spinal cord injury: a longitudinal study of mice, J. Neurotrauma (2024), https://doi.org/10.1089/neu.2023.0422.
[26] Q. Zhao, Y. Zhu, Y. Ren, S. Yin, L. Yu, R. Huang, S. Song, X. Hu, R. Zhu, L. Cheng, N. Xie, Neurogenesis potential of oligodendrocyte precursor cells from oligospheres and injured spinal cord, Front. Cell. Neurosci. 16 (2022) 1049562, https://doi.org/10.3389/fncel.2022.1049562.
[27] D.M. Basso, L.C. Fisher, A.J. Anderson, L.B. Jakeman, D.M. McTigue, P.G. Popovich, Basso Mouse Scale for locomotion detects differences in recovery after spinal cord injury in five common mouse strains, J. Neurotrauma 23 (2006) 635–659, https://doi.org/10.1089/neu.2006.23.635.
[28] V. Di Lazzaro, F. Pilato, M. Dileone, P. Profice, A. Oliviero, P. Mazzone, A. Insola, F. Ranieri, M. Meglio, P.J.T. Tonali, The Physiological Basis of the Effects of Intermittent Theta Burst Stimulation of the Human Motor Cortex, vol. 586, 2008, pp. 3871–3879.
[29] J.K. Kim, H.S. Park, J.S. Bae, Y.S. Jeong, K.J. Jung, J.Y.J.N. Lim, Effects of Multi-Session Intermittent Theta Burst Stimulation on Central Neuropathic Pain: a Randomized Controlled Trial, vol. 46, 2020, pp. 127–134.
[30] M.R. Hinder, E.L. Goss, H. Fujiyama, A.J. Canty, M.I. Garry, J. Rodger, J.J. Summers, Inter- and Intra-individual variability following intermittent theta burst stimulation: implications for rehabilitation and recovery, Brain Stimul. 7 (2014) 365–371, https://doi.org/10.1016/j.brs.2014.01.004.
[31] C. Watson, The somatosensory system, in: The Mouse Nervous System, 2012, pp. 563–570, https://doi.org/10.1016/b978-0-12-369497-3.10021-4.